Simulations of NMR experiments employing static and/or radio-frequency field gradients: application to slice selection by the inhomogeneous radio-frequency field of a standard coil

D. Canet, S. Leclerc, M. Rocher, F. Guenneau, D. Grandclaude

Simulations of NMR Experiments Employing Static and/or Radiofrequency Field Gradients. Application to Slice Selection by the Inhomogeneous Radiofrequency Field of a Standard Coil.

Daniel Canet, Sébastien Leclerc, Magali Rocher, Flavien Guenneau, and Denis Grandclaude

Laboratoire de Méthodologie RMN[‡], Université H. Poincaré, Nancy I, B.P. 239,
54506 Vandoeuvre-lès-Nancy (Cedex), France

[‡](UPRESA CNRS 7042, INCM-FR CNRS 1742)

Abstract. A general computer program has been developed in order to simulate any NMR experiment. It includes, in addition to the action of radiofrequency (rf) pulses and of gradients of both magnetic fields (static and rf), the effects of inhomogeneity of the latter. It has been used here for devising a slice selection procedure based on the inhomogeneity of the rf field delivered by a standard coil (e.g. a saddle-shaped coil). Two sequences have been investigated, a DANTE-like pulse train and a very simple one (named S^2P for Slice Selection with 2π pulses) , $[(2\pi)\text{-}\tau]_n$, where (2π) corresponds to the flip angle of the region to be selected whereas τ has to be chosen according to the relaxation time values; n, the number of cycles, must be sufficiently large, its actual value being uncritical. Simulations show that performances (in terms of selectivity) of both sequences are comparable while experimental verifications favor S^2P for its robustness and for the absence of any signal loss.

1. Introduction

Whenever one needs to select part of a sample, as this is for instance the case in conventional NMR two-dimensional imaging (the 2D image being that of a given slice), one generally resorts to a combination of static field (B_0) gradient (directed perpendicularly to the relevant slice) and of a frequency selective radio-frequency (rf) pulse [1]. However, B_0 gradients are known to suffer from magnetic susceptibility variations within the object under investigation (because of intrinsic heterogeneities or, more simply, because there is generally an abrupt change of magnetic susceptibility at the edges of the sample) [2]. These effects originate from gradients appearing at interfaces; they are thus proportional to the applied magnetic field and to the difference in magnetic susceptibilities. These gradients are of course superimposed to those used for imaging purposes and can therefore entail distortions or other unwanted effects (intensity losses, alteration of spatial resolution…). This superimposition of internal gradients with the imaging gradient is of course undesirable during phase and/or frequency encoding.

The alternative type of gradients used in NMR, namely gradients of the radio-frequency (rf) field (called B_1 gradients), have strengths comparable to those of B_0 gradients. However, because the B_1 field is much weaker (by several orders of magnitude) than the B_0 field, internal B_1 gradients are much weaker than those applied externally. This is one of the advantages of the B_1 gradients in addition to others which include short rise and fall times, the absence of eddy currents…[3] Inconveniences of these gradients are of course the difficulty to create very large gradients and to achieve encoding in the three spatial directions.

The goal of this paper is to present a general simulation method so as to be able to discuss various procedures based on B_1 gradients (or rather B_1 inhomogeneity of the standard coil used in the NMR probe for detection and for generating pulses of a rf field supposedly homogeneous). In fact, the rf field is never perfectly homogeneous and can be made purposely inhomogeneous in such a way that it should become feasible to select a zone corresponding to a given value of the rf field. The idea is

not new and essentially two types of approach have been proposed: DANTE-like [4] pulse trains [5-7] or composite pulses[8-11]. In this work, we shall focus on a DANTE-like sequence which has been used in this laboratory for some time and on a third approach which makes use of the repetition of a simple figure including a rf pulse and an evolution interval. To the best of our knowledge, such an approach has been attempted only once [12]. Finally, it should be mentioned that, although the methods which are described below have been developed for B_1-gradient imaging [13] (where the single turn coil which delivers the main gradient is perpendicular to the standard coil), they should be of general applicability in any situation requiring the selection of a slice perpendicular to the coil axis as for instance in solid state NMR [12, 14]

2. Simulations.

Several computer programs have been developed for simulating the evolution of spin systems under the application of B_0 gradients [15-17]. However, they do not take into account the intrinsic inhomogeneity of magnetic fields, which is needed in the present study. The only work [18] which treats this problem is directed toward specific applications related to the NMR-MOUSE [19] and does not involve B_0 or B_1 gradients which are essential here.

In the present situation where we try to devise a proper method without proceeding experimentally by trial and error, it is indeed advantageous to simulate the effects arising from the inhomogeneity of a rf field (having in mind that those effects should eventually lead to a slice selection procedure). To this end, we have written a computer program which calculates the NMR response from the characteristics of the pulse sequence and from the profile of the rf field along the axis of the corresponding coil. Actually, this software is very general, its description is purposely limited here to the behavior of a one-spin system (e.g. the water protons).

The pulse sequence can include:

1. Pulses of perfectly homogeneous rf field (hardly relevant in this study), characterized by their flip angle and phase (or phase cycle).
2. Pulses of the inhomogeneous rf field above mentioned (which will be essentially used here), characterized by the flip angle at the coil center (assumed to be maximum) and its phase (or phase cycle).
3. Evolution intervals with precession due either to chemical shift (in fact at a frequency corresponding to the difference between those of the signal and of the carrier; it will be denoted ν' in the following) or to B_0 inhomogeneity, the latter being characterized by an extra line broadening.
4. Pulses of B_0 gradients characterized by the maximum precession angle (within the sample). Precession due to chemical shift is superimposed to the precession arising from the gradient and the calculation of its effects requires obviously the pulse duration.
5. The phase of the acquisition, which will be useful in the case of phase cycling.

Moreover, the computer program can account for relaxation phenomena which proceed here only from the two relaxation times T_1 and T_2 whose values must therefore be entered.

B_1 inhomogeneity can be specified in two ways : i) by a series of number corresponding to B_1 values from the bottom to the top of the sample (measured experimentally), ii) or by a gaussian curve supposed to represent the B_1 evolution along the coil axis.

Homogeneous rf pulses amount to simple rotations of magnetization components around the appropriate axis of the rotating frame. For instance in the case of a pulse of flip angle α around the x axis of the rotating frame (phase: 0), magnetization components ($\mathbf{M}^+$ denotes magnetization after the pulse and $\mathbf{M}^-$ before the pulse) transform as :

$$
\begin{aligned}
M_x^+ &= M_x^- \\
M_y^+ &= M_y^- \cos(\alpha) + M_z^- \sin(\alpha) \\
M_z^+ &= -M_y^- \sin(\alpha) + M_z^- \cos(\alpha)
\end{aligned}
\tag{1}
$$

In the case of inhomogeneous rf pulses, the sample is decomposed into elementary slices, the flip angle being supposed perfectly determined for each of them and obtained from the B_1 profile (in practice, between 100 and 500 slices are defined). In fact, equations similar to (1) are used with a specific angle α (denoted by α_{slice}) which is calculated for each elementary slice :

$$
\alpha_{slice} = \frac{(B_1)_{slice}}{(B_1)_{\max}} \alpha_{\max} \tag{2}
$$

$(B_1)_{slice}$ is extracted from the list of B_1 values and $(B_1)_{max}$ is the maximum value in this list. $\alpha_{\max}$ is one of the inputs and corresponds generally to the flip angle at the coil center. The result for each slice is stored in an array so that it can be used as an initial state for the next event.

Of course, precession (due to chemical shift or to B_0 inhomogeneity) is again equivalent to a rotation but, this time, around the z axis. Magnetization components at the end of the precession interval ($\mathbf{M}^+$) can be expressed as a function of magnetization components at the beginning of the interval ($\mathbf{M}^-$). This is actually performed elementary slice by elementary slice to account for B_0 inhomogeneity. For speeding up calculations, these elementary slices can be made identical to those defined above for calculating B_1 inhomogeneity effects. However, for avoiding any spurious refocusing [20], it may be advisable to define two series of elementary slices. Let m_i^+ and m_i^- the corresponding magnetizations for the i^{th} elementary slice. One has :

$$
\begin{aligned}
m_{xi}^+ &= \left[\cos 2\pi\left(\nu' + \frac{wi}{n} - \frac{w}{2}\right)t\right] m_{xi}^- + \left[\sin 2\pi\left(\nu' + \frac{wi}{n} - \frac{w}{2}\right)t\right] m_{yi}^- \\
m_{yi}^+ &= -\left[\sin 2\pi\left(\nu' + \frac{wi}{n} - \frac{w}{2}\right)t\right] m_{xi}^- + \left[\cos 2\pi\left(\nu' + \frac{wi}{n} - \frac{w}{2}\right)t\right] m_{yi}^- \\
m_{zi}^+ &= m_{zi}^-
\end{aligned}
\tag{3}
$$

ν' is the precession frequency in the rotating frame. n is the number of elementary slices. w is the extra line width (at half height) due to B_0 inhomogeneity and is used for evaluating the relevant effects (the corresponding frequency range has been assumed to be twice this extra line width and therefore to be represented by the interval [$-w,+w$]).

The effect of B_0 gradient pulses is calculated in a similar way with generally a shorter value for the precession interval (in fact, the pulse duration is used only for evaluating the precession due to chemical shift). With m_i^+ and m_i^- the magnetization for each slice as defined above, one has :

$$\begin{aligned} m_{xi}^+ &= \left[\cos 2\pi\left(\nu'\tau + \frac{\beta i}{n} - \frac{\beta}{2}\right)\right] m_{xi}^- + \left[\sin 2\pi\left(\nu'\tau + \frac{\beta i}{n} - \frac{\beta}{2}\right)\right] m_{yi}^- \\ m_{yi}^+ &= -\left[\sin 2\pi\left(\nu'\tau + \frac{\beta i}{n} - \frac{\beta}{2}\right)\right] m_{xi}^- + \left[\cos 2\pi\left(\nu'\tau + \frac{\beta i}{n} - \frac{\beta}{2}\right)\right] m_{yi}^- \\ m_{zi}^+ &= m_{zi}^- \end{aligned} \qquad (4)$$

where τ is the pulse duration and [$-\beta/2,+\ \beta/2$] the angular range for the precession due to the gradient pulse.

Relaxation effects are still to be inserted; they are classically accounted for according to the Bloch equations, as we are supposedly dealing with systems which do not involve any cross-relaxation.

At the outcome, we have at hand the three magnetization components for each of the elementary slices in each of the series above defined. Possibly, a summation over one series can be performed yielding exclusively the effect of a given type of inhomogeneity (or of gradient). For instance, in order to assess slice selection by B_1 inhomogeneity, the effects of B_0 inhomogeneity must be averaged over the whole sample. These data are stored in appropriate files for further use with other software (Excel for instance) or displayed within this software. In particular, it will be useful here to visualize magnetization profiles along one spatial direction (which, in the present context, will be the direction along which B_1 is inhomogeneous). As, in most situations, the receiver coil is the coil which is used for slice selection (and which thus possesses a strong inhomogeneity), one must also

account for receptivity which, by virtue of the reciprocity principle, follows B_1 variations. Finally, if necessary, the total magnetization can be obtained by summing the contribution of all slices, taking possibly into account the coil receptivity.

This simulation software has been used i) for confirming the performances of a procedure which has been used for a long time in this laboratory (DANTE-like sequence), ii) for evaluating an even simpler procedure and also for optimizing its parameters. This is detailed in the next two subsections along with basic experimental results.

A DANTE-like sequence for slice selection.

The idea is to take the magnetization of the considered slice (located at the coil center) from the z axis to the y axis of the rotating frame by using a train of pulses of small flip angle. This method is widely used for spectral selectivity and is known under the acronym of DANTE [4]. For spatial (slice) selection, it can be adapted in the following way:

$$\left[(\alpha)_x(2\pi)_y\right]_n \text{ with } n\alpha = \pi/2 \qquad (5)$$

$(\alpha)_x$ and $(2\pi)_y$ refers to flip angles undergone by magnetization at the coil center. Of course for other regions, the flip angles are smaller in a such way that the $(\alpha)_x$ pulses have a cumulative effect only for magnetization at the coil center and take gradually this magnetization toward the y axis. Magnetizations for other regions lie somewhere in the xz plane and can be eliminated by phase cycling. Simulations have been performed with the B_1 profile existing for most experimental situations considered here (see experimental section). The result is shown in figure 1. The agreement of the simulation profile with the experimental one is seen to be very satisfactory except for the smaller side-lobes which could not be detected due to the fact that they tend to cancel each other (because the distance between two consecutive lobes is probably of the order of the spatial resolution).

The simplest slice selection procedure (S^2P for Slice Selection with 2π pulses).

We can now consider the following sequence which is probably the simplest we can think of in order to select a slice around the coil center:

$$\left[(2\pi)_x - \tau\right]_n \qquad (6)$$

As before, $(2\pi)_x$ refers in fact to the flip angle at the coil center, meaning that magnetization at other locations are subjected to a flip angle smaller than 2π, thus yielding transverse components during the time τ which may be destroyed by transverse relaxation and/or B_0 inhomogeneity. Repeating n times the building block (2π-τ) should lead to the suppression of this latter magnetization. By contrast, magnetization at the coil center is totally brought back to the z axis and therefore is not affected by any loss (relaxation or B_0 inhomogeneity). τ should not be too long in order to prevent too much reconstruction by longitudinal relaxation. In any case, slice selection should improve in a certain extent with the numbers of cycle n. As usual, we have compared in figure 2 experimental and simulated profiles for the following parameters : T_1=T_2=3s, T_2^*=0.05s, which are typical for a sample filled with water. Globally, the two traces are quite consistent except, again, for the side-lobes. Various simulations have been performed showing first that the effects of a short natural T_2 are almost identical to those obtained with B_0 inhomogeneity (T_2^*), meaning that no (or negligible) refocusing occurs as it would be the case with a train of π pulses. In order to attain a good selection, τ must be set to a small value adapted to the relaxation times, as shown by numerous simulations performed with various sets of relaxation times. It turns out that side lobes exist (as in the DANTE-like sequence); however, they drop considerably and even almost disappear when the number of cycles n is increased (see the simulations of figure 3). Moreover, this parameter beyond a sufficient value is by no way critical. Now, one may wonder why S^2P works and whether transverse relaxation (natural or effective) plays the dominant role as believed intuitively. In fact, it suffices to

consider regions where the flip angle is π (2π for the slice of interest) to be perfectly convinced that T_1 is as well important. Recovery of longitudinal magnetization is governed by

$$m_z(t) = m_0 + [m_z(0) - m_0]\exp(-t/T_1) \qquad (7)$$

where m_0 is the equilibrium magnetization of the considered region and $m_z(0)$ the longitudinal magnetization at the beginning of the evolution period. T_1 will be active proportionally to the difference $[m_z(0) - m_0]$. This means that the effect of T_1 is smaller when longitudinal magnetization is positive. Since for a π flip angle, longitudinal magnetization alternates between positive and negative values, it will finally tends to zero because, when it is negative, the second term in (7) pushes it toward zero more effectively than it pushes it toward its equilibrium value whenever longitudinal magnetization is positive. This brief discussion shows that a subtle interplay occurs between T_1 and T_2 effects and that, in practice, simulations will be necessary for determining the optimal values of τ and n in the S^2P sequence. Simulations have also shown that transverse magnetization is still present by the end of the pulse train. Elimination of these transverse components is easily achieved by phase cycling or, better, by a B_0 gradient pulse.

3. Additional experimental results.

All experiments have been performed with a home-made 200 MHz spectrometer equipped with a wide-bore Oxford magnet. A probe designed for B_1 gradient imaging has been used [13]. It consists of a two-turn coil which generates the imaging gradient (around 15 G/cm) and of a saddle shaped coil (orthogonal to the latter, devoted to signal detection and to slice selection) with a diameter and height of 8mm. The proton NMR signal of water in sample tubes of 3mm o.d. have been measured throughout. Rapid imaging (acquisition between short pulses of B_1 gradient) [21] yields one-dimensional (and in-plane) images which corresponds to a projection perpendicularly to the gradient direction. Because other gradient directions are not available, the sample is rotated step

by step leading to a new projection at each step. From a whole set of projections, a two dimensional image can be reconstructed by an algorithm related to the Filtered-back-projection method.

The one-dimensional image of a tube filled with water is shown in figure 4 without and with slice selection; in that case, it can be seen that the expected semi-circular aspect is obtained only when applying slice selection procedures. The actual experimental device for obtaining the selection profile along the Z direction (see for instance figures 1 and 2) is a Shigemi tube [22] involving a piston whose magnetic susceptibility is identical to the one of water and which is used to limit a water layer at a desired thickness (here less than 1 mm); the water layer is moved along the Z axis prior to each new experiment. Unfortunately, unavoidable residual water between the piston and the tube wall produces some artifacts (imperfections mentioned in the legends of the figures). The usefulness of slice selection is further illustrated by the two Z-profiles (with and without slice selection) shown in figure 5.

4. Conclusion.

We have shown that slice selection can be achieved by resorting to the inhomogeneity of the rf field delivered by a standard NMR coil. Among the various possibilities, it turns out that the novel (and very simple) methodology presented here (the S^2P sequence) is especially appealing. It is quite robust since it just requires the length of the 2π pulse at the coil center, parameter which appears, for this sequence, much less critical than in the case of the DANTE-like sequence. Concerning selectivity itself, performances are quite comparable although the profile shapes are a little different: triangular for S^2P, more rectangular for the DANTE-like sequence (figure 6). However a decisive advantage of S^2P lies in its very favorable sensitivity, as compared with the DANTE-like sequence (contrary to what is seen in figure 6, where the two profiles were normalized with respect to each other). The latter undergoes a considerable signal loss (by at least a factor 3) probably by relaxation and/or by experimental artifacts. Finally, we present in figure 7 an

illustrative, though preliminary, example of the efficiency of slice selection as achieved by the S^2P method. It must be mentioned that such results do not require particular efforts and should be obtained in the future on a routine basis. Of course, the performances of the slice selection procedures presented in this paper do not compare, at the present time, with those based on B_0 gradient methodology. However their merit arises from two features: i) they do not require any special equipment, ii) they are free from the inherent disadvantages of B_0 gradients, in terms of magnetic susceptibility differences within the object under investigation. Moreover, slice selection using the S^2P method should be improvable. Two approaches could be considered : i) a decrease of the coil height to further reduce the slice thickness, ii) some modulation of the pulse train to obtain a more rectangular shape. For both, the simulation software described in this paper should be especially useful and avoid repetitive and tedious experiments based on trial and error.

References

[1] Callaghan P.T.: “Principles of Magnetic Resonance”. Oxford : Clarendon Press 1991.

[2] Blümich B.: “NMR imaging of materials”. Oxford : Clarendon Press 2000.

[3] Canet D.: Prog. NMR Spectrosc. **30**, 101 (1997)

[4] Morris G., Freeman R.: J. Magn. Reson. **29**, 422 (1978)

[5] Karczmar G.S., Lawry T.J., Weiner M.W., Matson G.B.: J. Magn. Reson. **76**, 41 (1988)

[6] Maffei P., Elbayed K., Brondeau J., Canet D.: J. Magn. Reson. **95**, 392 (1992)

[7] Kaczynski J., Dodd N.J.F., Wood B.: J. Magn. Reson. **100**, 453 (1992)

[8] Shaka A.J., Freeman R.: J. Magn. Reson. **59**, 169 (1984)

[9] Tycko R., Pines A.: J. Magn. Reson. **60**, 156 (1984)

[10] Scheffler K.: J. Magn. Reson. B **109**, 175 (1995)

[11] Kemp-Harper R., Styles P., Wimperis S.: J. Magn. Reson. A **123**, 230 (1996)

[12] Charmont P.: PhD thesis, Ecole Nomale Supérieure de Lyon 2000.

[13] Boudot D., Montigny F., Elbayed K., Mutzenhardt P., Diter B., Brondeau J., Canet D.: J. Magn. Reson. **92**, 605 (1991)

[14] Charmont P., Lesage A., Steuernagel S., Engelke F., Emsley L.: J. Magn. Reson. **145**, 334 (2000)

[15] Jerschow A., Muller N.: J. Magn. Reson. **134**, 17 (1998)

[16] Meresi G.H., Cuperlovic M., Palke W.E., Gerig J.T.: J. magn. Reson. **137**, 186 (1999)

[17] Nicholas P., Fushman D., Ruchinsky V., Cowburn D.: J. Magn. Reson. **145**, 262 (2000)

[18] Balibanu F., Hailu K., Eymael R., Demco D.E., Blümich B.: J. Magn. Reson. **145**, 246 (2000)

[19] Eidmann G., Salvesberg R., Blümer P., Blümich B.: J. Magn. Reson. **122**, 104 (1996)

[20] Ardelean I., Scharfenecker A., Kimmich R.: J. Magn. Reson. **144**, 45 (2000)

[21] Boudot D., Canet D., Brondeau J.: J. Magn. Reson. **87**, 385 (1990)

[22] Symmetrical microtube matched with D2O, SHIGEMI Co. Ltd, Tokyo

Figure captions

Figure 1 : Comparison of experimental and simulated profiles corresponding to a slice selection obtained with the DANTE-like sequence for n=10. The horizontal scale corresponds to the axis of the rf coil, the origin coinciding with the coil center. The right part of the experimental trace involves an unwanted signal due to imperfections of the experimental device.

Figure 2 : Comparison of experimental and simulated profiles corresponding to a slice selection obtained with the S^2P sequence for τ=0.1s, n=100 (T_1=T_2=3s, T_2^*=0.05s). The shoulder at the right part of the experimental trace is again due to the same type of imperfections as those mentioned in figure 1 (results of figures 1 and 2 have been obtained with different test samples).

Figure 3 : Simulated profiles corresponding to the S^2P sequence (T_1=T_2=3s, T_2^*=0.5s, τ = 0.2s) for n=10 (right) and n=50 (left).

Figure 4 : One-dimensional images of an NMR tube with and without slice selection.

Figure 5 : Comparison of profiles with and without slice selection. The latter actually provides the B_1 profile along the Z direction (saddle coil axis).

Figure 6 : Comparison of experimental profiles obtained with S^2P and DANTE-like sequences (extracted from figures 1 and 2). Only the left part is meaningful, imperfections of the experimental device affecting the right part.

Figure 7 : Two-dimensional images of the object (filled with water) shown at the bottom of the figure (3mm o.d. sample tube).
Top left: with slice selection, where the glass bead appears. The shape of this dark zone as well as its non-uniformity is due to the fact that a slight amount of water is selected above and under the bead.
Top right: without slice selection, where water above and under the glass bead contributes to suppress the dark zone corresponding to the glass bead. The small residual dark zone corresponds to the junction between the capillary and the bead

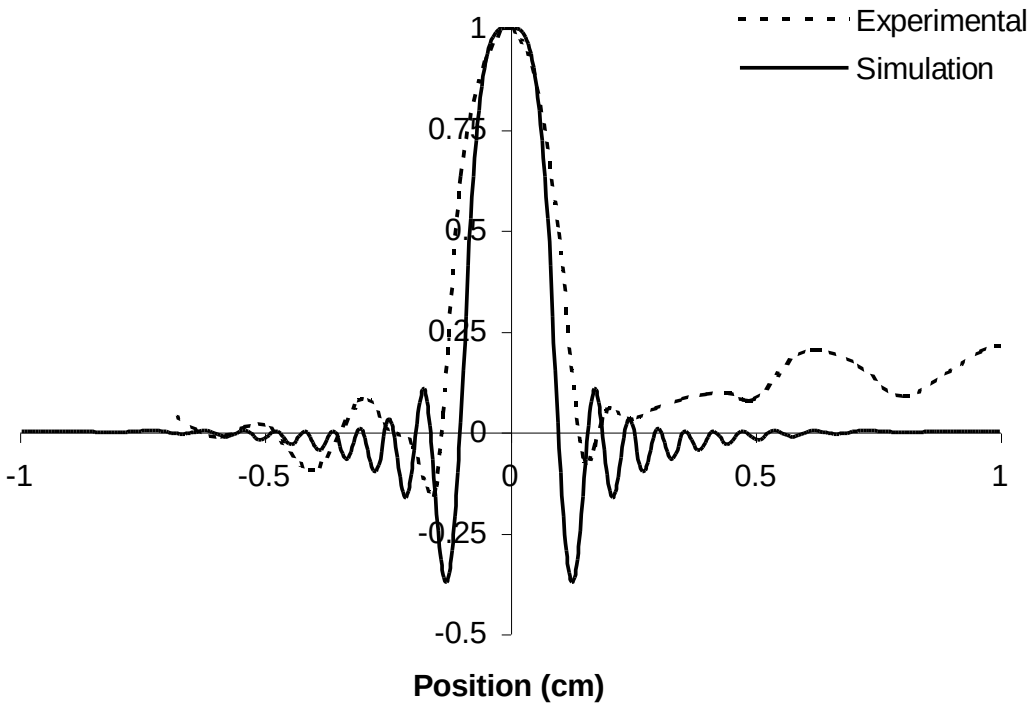
Experimental
Simulation
1
0.75
0.5
0.25
0
-0.25
-0.5
-1
-0.5
0
0.5
1
Position (cm)

Figure 1

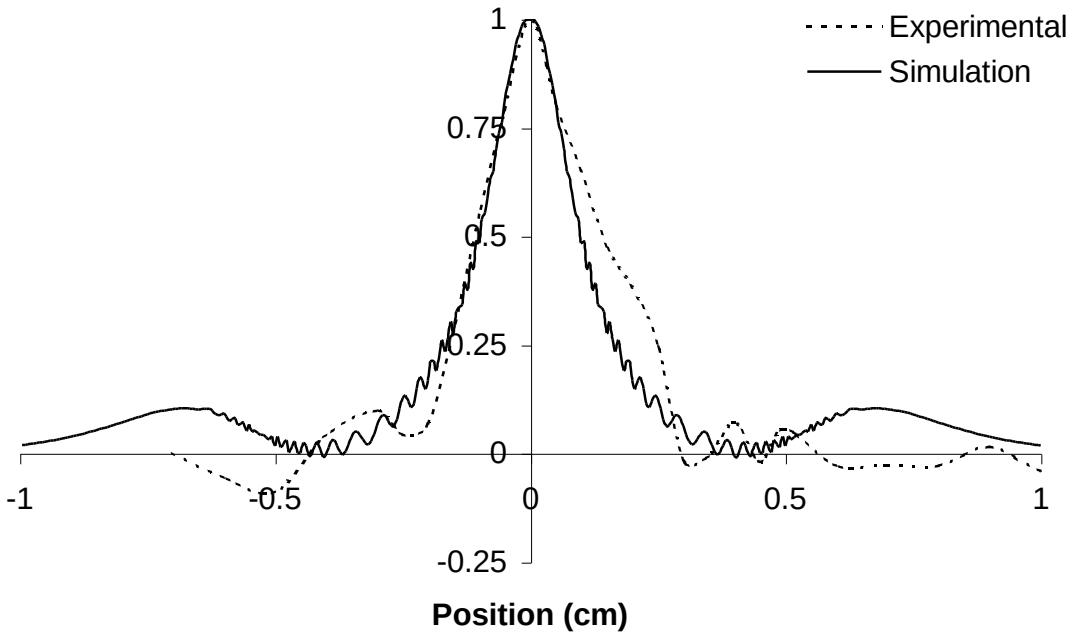
Experimental
Simulation
1
0.75
0.5
0.25
0
-0.25
-1
-0.5
0
0.5
1
Position (cm)

Figure 2

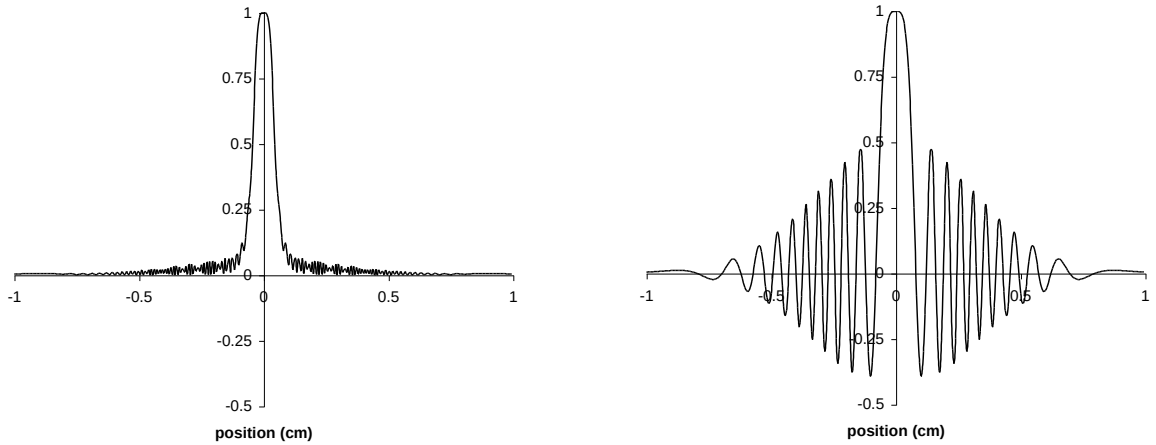
1
0.75
0.5
0.25
0
-0.25
-0.5
-1
-0.5
0
0.5
1
position (cm)
1
0.75
0.5
0.25
0
-0.25
-0.5
-1
-0.5
0
0.5
1
position (cm)

Figure 3

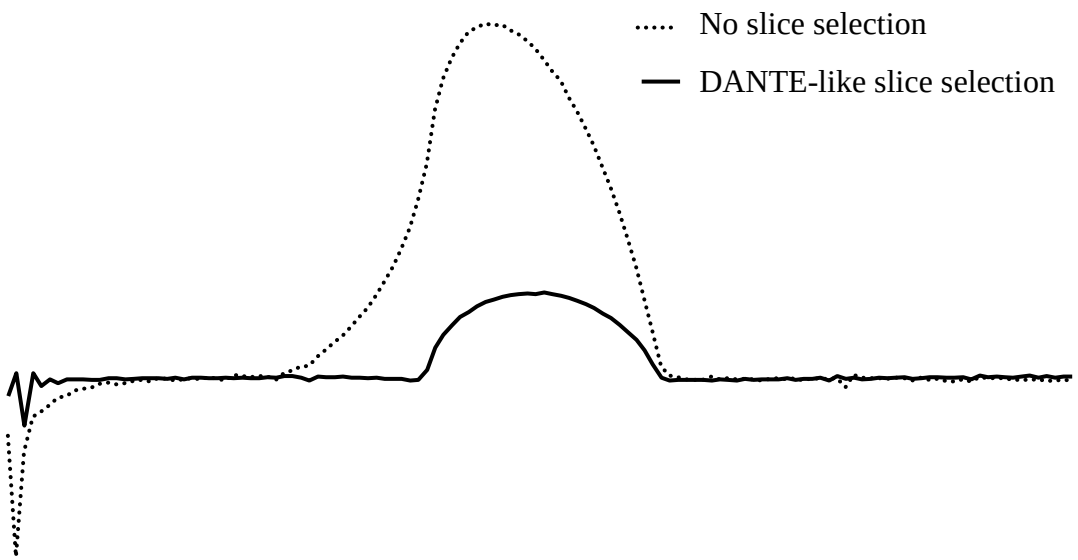

Figure 4

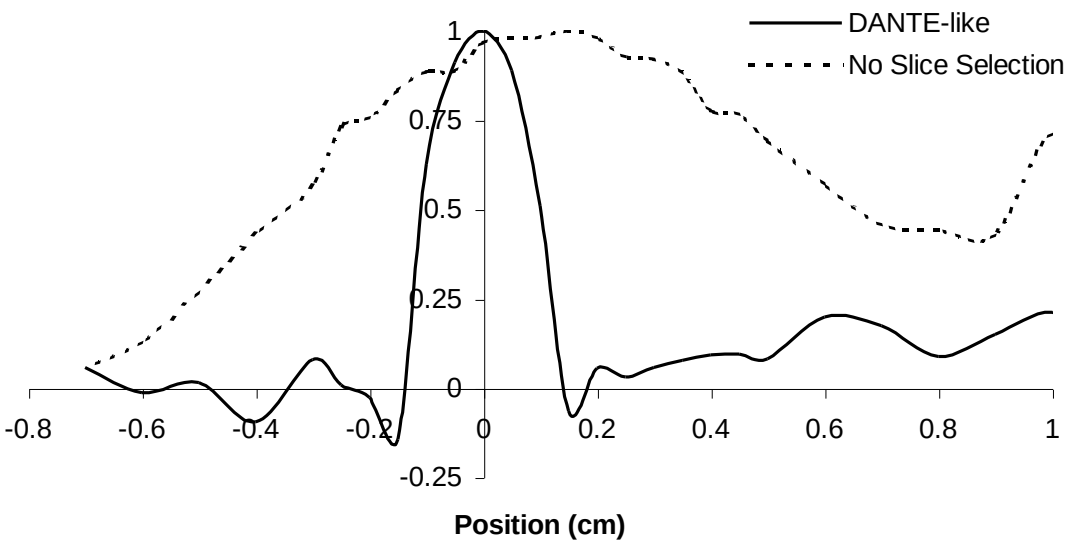
DANTE-like
No Slice Selection
1
0.75
0.5
0.25
0
-0.25
-0.8
-0.6
-0.4
-0.2
0
0.2
0.4
0.6
0.8
1
Position (cm)

Figure 5

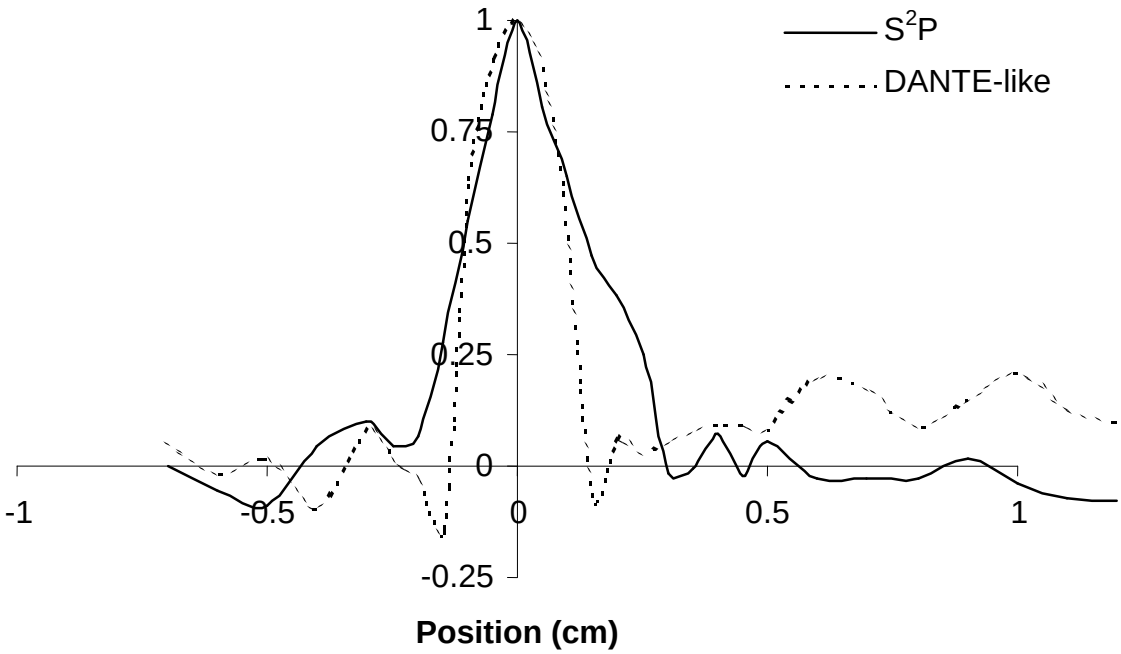

Figure 6

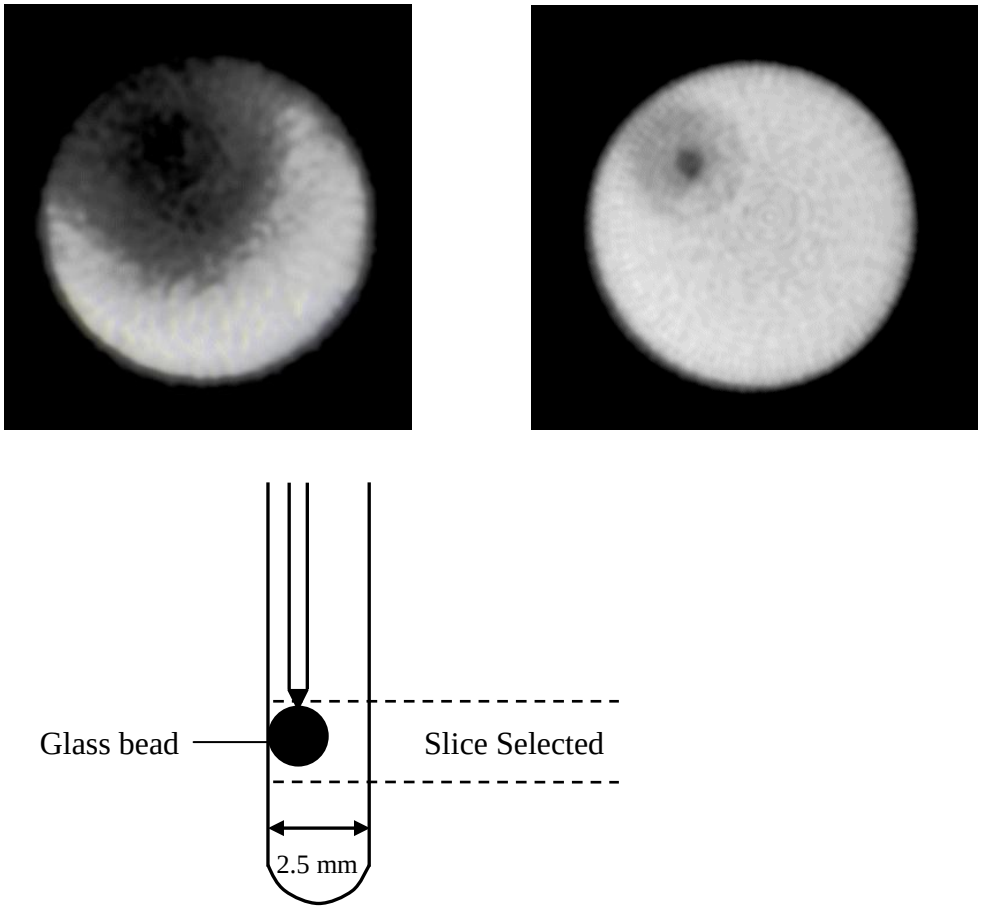

Figure 7